Thermochimica Acta, 164 (1990) 21-36
Elsevier Science Publishers B.V., Amsterdam

THERMAL BEHAVIOR OF SOME Ni^{II} AND Fe^{III} SALTS

AHMED M. GADALLA * and HSUAN-FU YU

Chemical Engineering Department, Texas A&M University, College Station, TX 77843 (U.S.A.)

(Received 26 October 1989)

ABSTRACT

The intermediate phases and reactions during the thermal decomposition of nitrates and acetates of Ni^{II} and Fe^{III} as well as their mixtures were established using thermal analysis and X-ray diffraction. The thermal analyses were conducted in stagnant and flowing air using different heating rates. The results were also compared with those for Ni^{II} and Fe^{III} hydroxides.

INTRODUCTION

An understanding of the thermal behavior of Ni^{II} and Fe^{III} salts is relevant to the production of nickel ferrite. Because the traditional preparation of ferrite by solid-state reaction of mixed oxide powders has reached its limits, several novel processes exploiting liquid or vapor phases as well as aerosol-phase preparation are under investigation and development. Aerosol techniques allow production of fine droplets, each droplet comprising the constituents mixed on an atomic scale. Pyrolysis of these droplets causes rapid reaction and formation of spherical particles with controlled morphology. In the aerosolization process, the choice of starting materials which can provide reliably homogeneous systems and have low decomposition temperatures is crucial to the success of the process. In this study, the thermal behavior of nitrates and acetates of Ni^{II} and Fe^{III} was examined. The results were also compared with those for the hydroxides previously obtained in this laboratory.

PREVIOUS WORK

Nickel nitrate hexahydrate

Several intermediate compounds were reported to develop during thermal analysis of nickel nitrate hexahydrate but there is no agreement regarding

---

* Author to whom correspondence should be addressed.

0040-6031/90/$03.50

the nature of these intermediates. Wendlandt [1] reported that, with a heating rate of 5.4 °C min^{-1} in flowing air, nickel nitrate hexahydrate decomposed to NiO at 505 °C and anhydrous $Ni(NO_3)_2$ was formed at 205 °C as an intermediate compound. On the other hand, Dollimore et al. [2,3] and Criado et al. [4] reported that in stagnant air, basic nickel nitrates appeared as intermediates. Dollimore et al. [5] reported that with a heating rate of 0.8 °C min^{-1} in a vacuum, the nitrate started to decompose at about 127 °C and above 227 °C, $Ni(OH)_2$ was observed. On the other hand, Criado et al. [4] reported the existence of the anhydrous salt as the vacuum intermediate product.

In a water vapor–air medium, with heating rates of 5–7 °C min^{-1}, Kalinichenko and Purtov [6] reported that hexahydrate decomposed to NiO with the following intermediate phases: $Ni(NO_3)_2 \cdot 4H_2O$, $Ni(NO_3)_2 \cdot 3H_2O$, and $xNi(NO_3)_2 \cdot yNi(OH)_2 \cdot zH_2O$, where $y \approx 1.16$, and x and z were unspecified constants. In nitrogen flowing at a rate of 80 cm^3 min^{-1} and with a heating rate of 1 °C min^{-1}, the intermediates reported by Mu and Perlmulter [7] were $Ni(NO_3)_2 \cdot nH_2O$ were $n = 4.5$, 3, 1.5, and 0. NiO was obtained at pyrolysis temperature above 350 °C.

Iron(III) nitrate nonahydrate

Wendlandt [1] reported that iron nitrate nonahydrate began to lose its water of hydration at 35 °C in flowing air when a heating rate of 5.4 °C min^{-1} was used. The thermal decomposition proceeded directly to Fe_2O_3 which was obtained at 445 °C. On the other hand, Mu and Perlmutter [7] stated that this salt decomposed to Fe_2O_3 after heating up to 280 °C in flowing nitrogen at a heating rate of 1 °C min^{-1}; they reported the existence of anhydrous iron nitrate as an intermediate phase during the decomposition.

Nickel acetate tetrahydrate

Leicester and Redman [8] reported that, in air, nickel acetate tetrahydrate began to lose its water of crystallization at about 70 °C, and the anhydrous material began to decompose at about 260 °C. Below 450 °C, NiO with excess oxygen was obtained, but above this temperature the weight of the residue was less than that expected for the oxide. Above 520 °C a gain in weight was observed at the end of the decomposition, implying oxidation of nickel metal.

Dollimore and Pearce [9] studied the decomposition of the salt in air using a heating rate of 4 °C min^{-1}. They reported that the tetrahydrate decomposed to anhydrous nickel acetate in the temperature range from 403 to 493 °C and that NiO first appeared at 623 °C. Baraldi [10] stated that, in air, the salt started to dehydrate at about 95 °C and NiO was obtained between 160 and 230 ° C. No intermediate was reported. In vacuum, the salt began to lose its water of crystallization at 80 ° C, and Ni and NiO were obtained at 275–300 ° C.

Basic iron(III) acetate

Music et al. [11] reported that at 150 ° C, basic ferric acetate decomposed to α- and γ-Fe_2O_3, but above 600 ° C only α-Fe_2O_3 was found.

Thermal analysis of mixed salts

Nothing has been reported in the literature regarding the thermal decomposition of mixed nitrates or acetates. The study on the thermal behavior of these mixed salts is reported for the first time in the present work.

EXPERIMENTAL TECHNIQUES

The thermal analysis was carried out using a Netzsch Simultaneous Thermal Analyzer, STA 409, which is capable of performing differential thermal analysis (DTA) and thermogravimetry (TG) simultaneously for the same sample. All studies were conducted in stagnant and flowing (10.9 ml min^{-1}) air using different heating rates. The materials investigated included nickel nitrate hexahydrate of 99.7% purity, iron nitrate nonahydrate of 98% purity, technical grade nickel acetate tetrahydrate, and dry basic ferric acetate. The nitrates and nickel acetate were purchased from AESAR; ferric acetate was purchased from Stagent–Welch Scientific Company. Calcined kaolin was used as a reference material and alumina crucibles of 99.5% purity were used as sample holders. The intermediate phases and reactions were concluded from the information obtained from TG, DTA, their first derivatives, and X-ray diffraction.

RESULTS AND DISCUSSION

Nickel nitrate hexahydrate

Figure 1 shows the thermal curves for $Ni(NO_3)_2 \cdot 6H_2O$ obtained in stagnant air using a heating rate of 1° C min^{-1}. A constant weight was achieved above 350 ° C after losing 73.33% of the original weight. This constant weight indicated that NiO had been formed. This conclusion was confirmed by X-ray diffraction of the specimens collected at 600 and

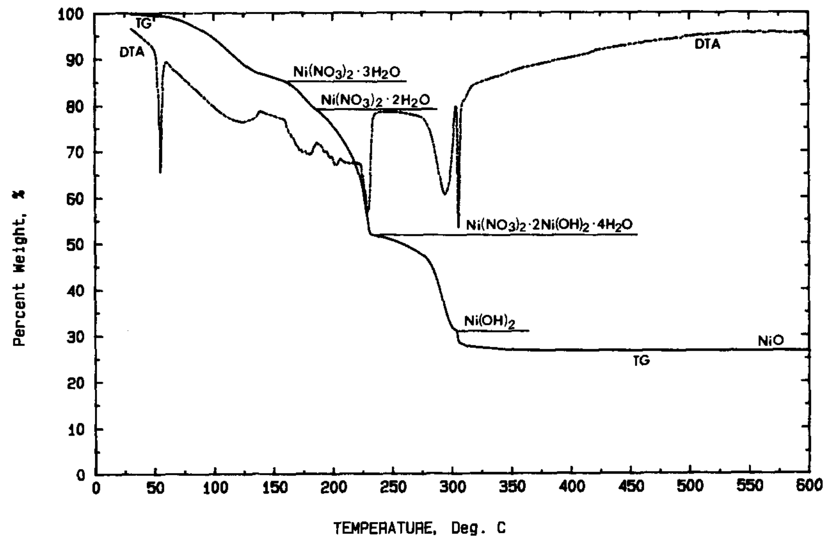

Fig. 1. Thermal analysis of nickel nitrate hexahydrate in stagnant air.

1100 °C. The X-ray patterns indicated the presence of well crystallized NiO and also showed that high temperature caused rapid grain growth as demonstrated by the decrease in the broadness of the peaks.

Using the final weight obtained to represent NiO, a back calculation indicated that the initial composition of the salt was not $Ni(NO_3)_2 \cdot 6H_2O$ but $Ni(NO_3)_2 \cdot 5.4H_2O$. The discrepancy can be attributed to a partial loss of water of crystallization during transportation and/or storage. This conclusion was based on observing the weight loss starting at 35 °C (Fig. 1).

A sharp endothermic peak followed by a gradual loss in weight started at about 50 °C. This indicated that the hydrate decomposed (at least partly) below the boiling point of water giving liquid water which started to evaporate yielding a second endothermic peak corresponding to the latent heat of vaporization. The rate of evaporation reached its maximum at about 120 °C. After reaching a composition corresponding to $Ni(NO_3)_2 \cdot 3H_2O$ (on the TG curve), a second progressive loss in weight occurred between 160 and 185 °C giving a composition corresponding to $Ni(NO_3)_2 \cdot 2H_2O$. The latter decomposed with an accelerated rate between 185 and 233 °C. At 233 °C the composition approached that of basic nickel nitrate tetrahydrate, $Ni(NO_3)_2 \cdot 2Ni(OH)_2 \cdot 4H_2O$. Then, it decomposed with an accelerated rate reaching its maximum at 293 °C until a small plateau on the TG curve was observed at about 303 °C. This arrest corresponded to the composition of $Ni(OH)_2$ which decomposed to NiO. Above 350 °C, the weight of the salt approached that corresponding to stoichiometric NiO.

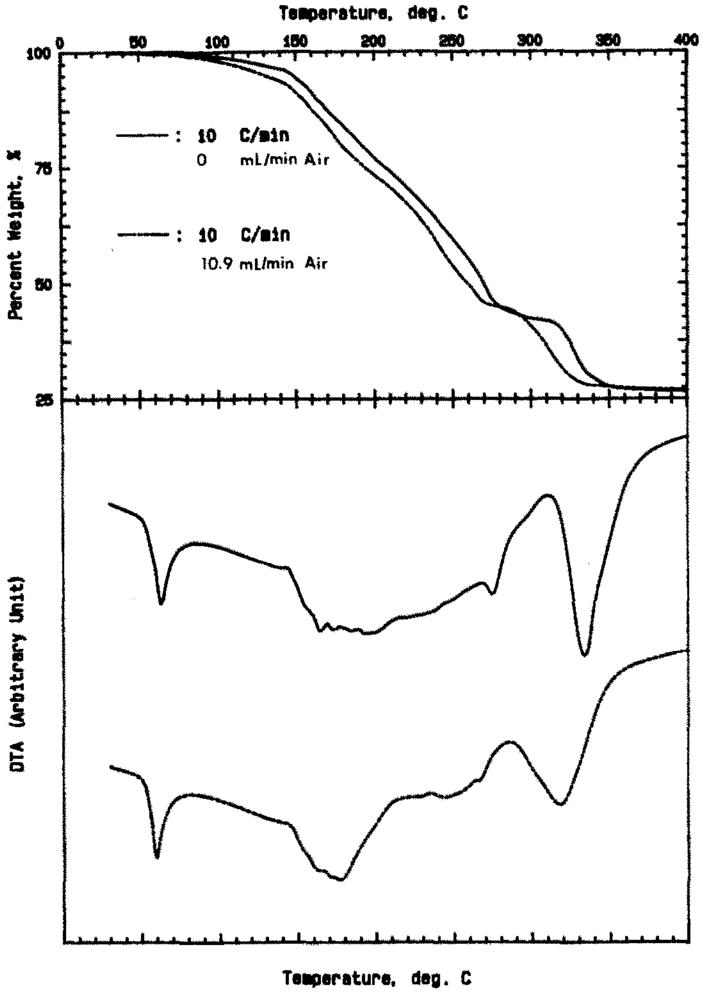

Fig. 2. Effect of flowing air on the decomposition of nickel nitrate hexahydrate.

The decomposition mechanism of nickel nitrate hexahydrate with the above conditions (stagnant air and 1° C min^{-1} heating rate) is thus

$$\mathrm{Ni(NO_3)_2 \cdot 6H_2O} \xrightarrow[-3\mathrm{H_2O}]{} \mathrm{Ni(NO_3)_2 \cdot 3H_2O} \xrightarrow[-\mathrm{H_2O}]{} \mathrm{Ni(NO_3)_2 \cdot 2H_2O}$$

$$\xrightarrow[-2/3\mathrm{N_2O_5}]{} \tfrac{1}{3}\{\mathrm{Ni(NO_3)_2 \cdot 2Ni(OH)_2 \cdot 4H_2O}\} \xrightarrow[-\mathrm{H_2O},\,-1/3\mathrm{N_2O_5}]{}$$

$$\mathrm{Ni(OH)_2} \xrightarrow[-\mathrm{H_2O}]{} \mathrm{NiO} \qquad (1)$$

When a stream of air was introduced, all the decomposition reactions occurred at lower temperatures (Fig. 2) due to the enhanced removal of the gaseous by-products by the air stream. Increasing the heating rate caused the elevation of the decomposition temperatures and the broadening of the peaks on the DTA curves (Fig. 3), essentially due to a decrease in the

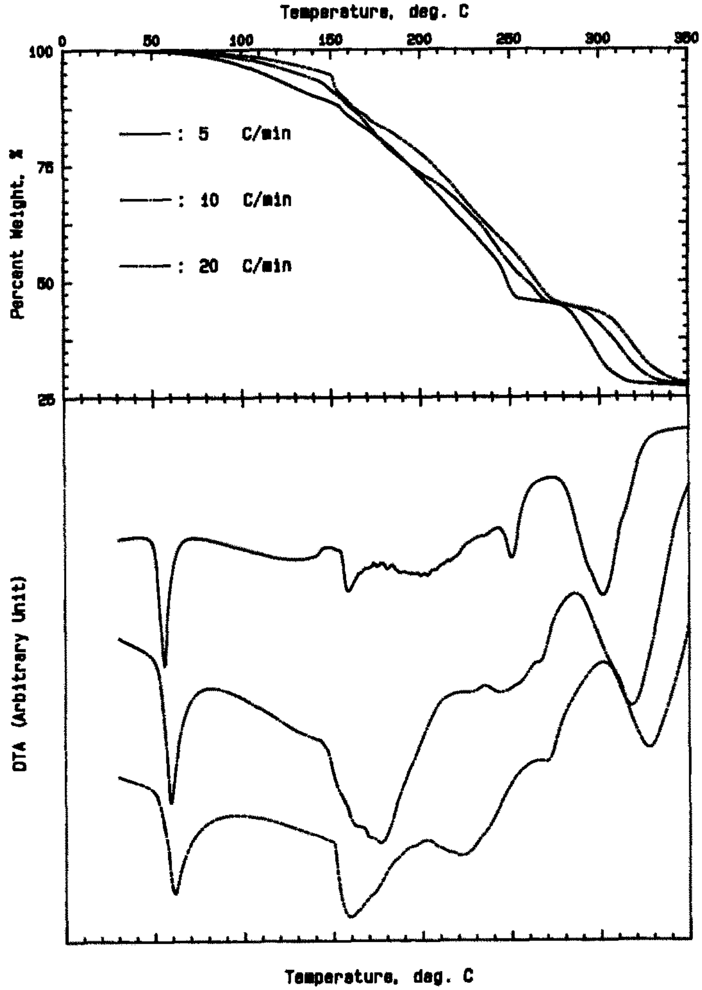

Fig. 3. Effect of heating rate on the decomposition of nickel nitrate hexahydrate in flowing air (10.9 ml $\min^{-1}$).

homogeneity of the temperature inside the material. A point of interest was that all the curves obtained with heating rates of 5 °C $\min^{-1}$ and above were similar, but were different from those obtained with a heating rate of 1 °C $\min^{-1}$. Faster rates showed an initial acceleration of weight loss which did not slow down at about 135 °C as occurred with the lower heating rate (Fig. 1). No indication for the complete loss of water, formation of $Ni(NO_3)_2 \cdot 3H_2O$, or its decomposition at 160 °C, was observed. With faster heating rates, the loss of liquid water at 60–70 °C was accelerated by heating and at 150 °C a faster drop in weight was observed and the rate continued to accelerate. A new endothermic peak appeared at 150 °C. This implies that the remaining liquid water boiled at 150 °C. The elevation in boiling point indicates that the nitrate dissolves in the water formed by the decomposition. The distinct breaks, discussed for 1° C min^{-1} heating, corresponding to $Ni(NO_3)_2 \cdot 3H_2O$, $Ni(NO_3)_2 \cdot 2H_2O$ and $Ni(NO_3)_2 \cdot 2Ni(OH)_2 \cdot 4H_2O$, were not detected at higher heating rates. The nearly horizontal line observed in Figs. 2 and 3 corresponds to $Ni(NO_3)_2 \cdot 2Ni(OH)_2$. This anhydrous basic nitrate decomposed directly to NiO except at the heating rate of 5° C min^{-1}. The peak at 250° C obtained at 5° C min^{-1} may correspond to the decomposition of $Ni(NO_3)_2 \cdot 2Ni(OH)_2 \cdot 4H_2O$ to $Ni(NO_3)_2 \cdot 2Ni(OH)_2$. However, at higher heating rates, this peak broadened and became difficult to distinguish (Fig. 3). It seems that the heating rate of 1° C min^{-1} revealed several intermediate products and higher rates caused the overlap of the corresponding decomposition reactions revealing only the anhydrous basic nitrate which was not detected at the lowest rate investigated.

Iron(III) nitrate nonahydrate

Figures 4 and 5 summarize the thermal curves obtained for $Fe(NO_3)_3 \cdot 9H_2O$. A flow of air or lower heating rates shifted the decomposition temperatures to lower values. The composition above 250° C corresponded to Fe_2O_3, as proved by X-ray analyses at 600 and 1100° C. Using the weight obtained at 500° C to corrrespond to stoichiometric Fe_2O_3, a back calculation indicated that the initial composition was not $Fe(NO_3)_3 \cdot 9H_2O$ but $Fe(NO_3)_3 \cdot 8.7H_2O$. The cause of this discrepancy was the same as that for nickel nitrate mentioned above and was evident from the TG curve which indicated that loss in weight began at 50° C.

All the DTA curves revealed an endothermic peak starting at about 50° C corresponding to partial decomposition of the hydrate, giving liquid water. Above this temperature, water was lost at an accelerated rate until a break corresponding to the composition of iron nitrate dihydrate, $Fe(NO_3)_3 \cdot 2H_2O$, was reached. The dihydrate decomposed at another accelerated rate (appearing as a nearly vertical step on the TG curves). The end of this step corresponded to the composition of $Fe_2O_3 \cdot 3H_2O$ and was accompanied by an endothermic peak (on the DTA curves). This peak was due to a combined loss of nitrogen oxides and water vapor. Increasing the temperature caused the gradual dehydration of $Fe_2O_3 \cdot 3H_2O$ and then the formation of anhydrous Fe_2O_3 causing the TG curves to level to a constant weight. No evidence for the existence of an anhydrous iron nitrate, as intermediate, was found in this study. Accordingly, the decomposition of iron nitrate nonahydrate follows the following steps

$$Fe(NO_3)_3 \cdot 9H_2O \xrightarrow[-7H_2O]{} Fe(NO_3)_3 \cdot 2H_2O$$

$$\xrightarrow[-3/2N_2O_5,\ -1/2H_2O]{} \tfrac{1}{2}Fe_2O_3 \cdot 3H_2O \xrightarrow[-3/2H_2O]{} \tfrac{1}{2}Fe_2O_3 \qquad (2)$$

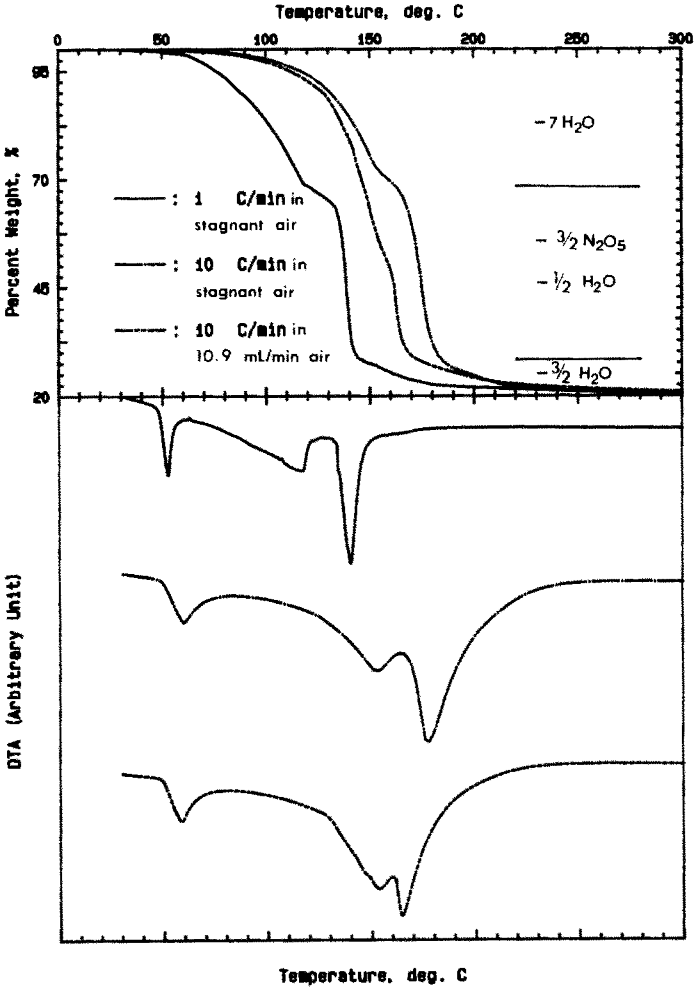

Fig. 4. Thermal curves of iron nitrate nonahydrate.

If the salt is heated further, up to 1500 ° C, a small endothermic peak can be detected on the DTA curve at temperatures between 1372 and 1400 ° C. The endothermic reaction is accompanied by a slight reversible weight loss and is due to the decomposition of Fe_2O_3 to magnetite of composition Fe_3O_{4+x}. A phase diagram published for $FeO-Fe_2O_3$ [12] indicates beyond any doubt that Fe_2O_3 decomposes in air to a non-stoichiometric magnetite which is rich in oxygen and has a composition of about $Fe_3O_{4.09}$ at 1400 ° C.

Mixed nitrates

Figure 6 shows the results of thermal analyses for the mixed nitrates which were carried out in stagnant air using different heating rates. After

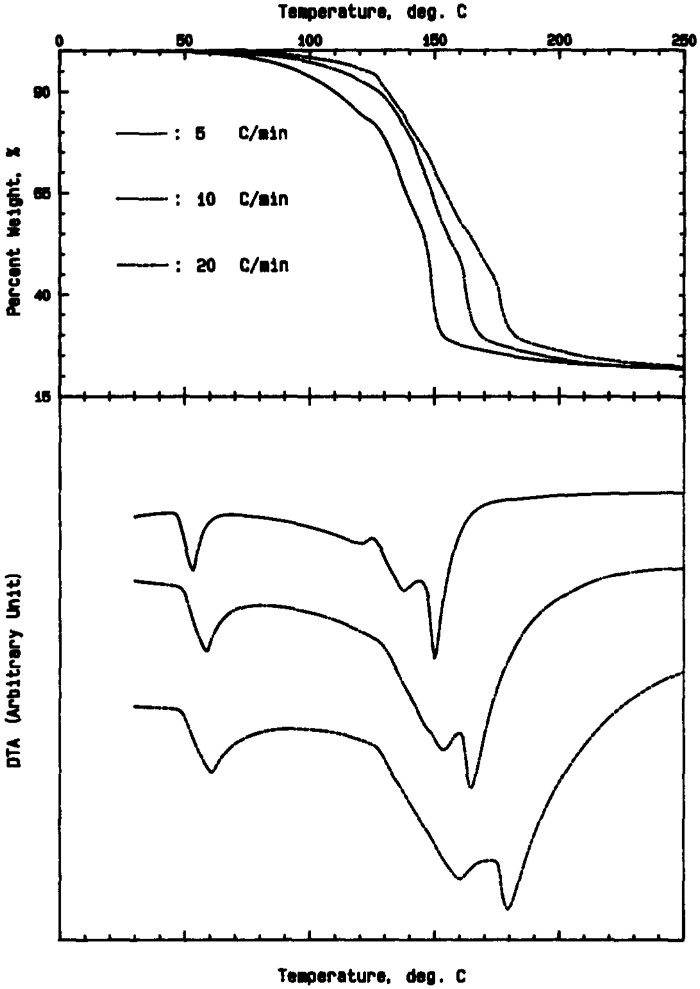

Fig. 5. Effect of heating rate on the decomposition of iron nitrate nonahydrate in flowing air (10.9 ml min^{-1}).

heating the mixed nitrates up to 500 °C, a total weight loss of 78% was observed. This weight loss agreed with the theoretical weight loss, 78.27%, to form $NiFe_2O_4$.

Several endothermic peaks appeared on the DTA curve for the mixture. The DTA curves for the mixture were overlaps of the individual curves. The first double peaks observed (for heating rate 1 °C min^{-1}) at temperatures between 30 and 57 °C represented the successive decomposition of the two hydrates giving liquid water. Then there was a weight loss at an accelerated rate giving an endothermic peak in the temperature range from 57 to 114 °C. The nitrate began to decompose giving nitrogen oxides at about 115 °C. This decomposition occurred between 115 and 160 °C and was accompanied by a sharp endothermic peak on the DTA curve and a rapid weight loss on the

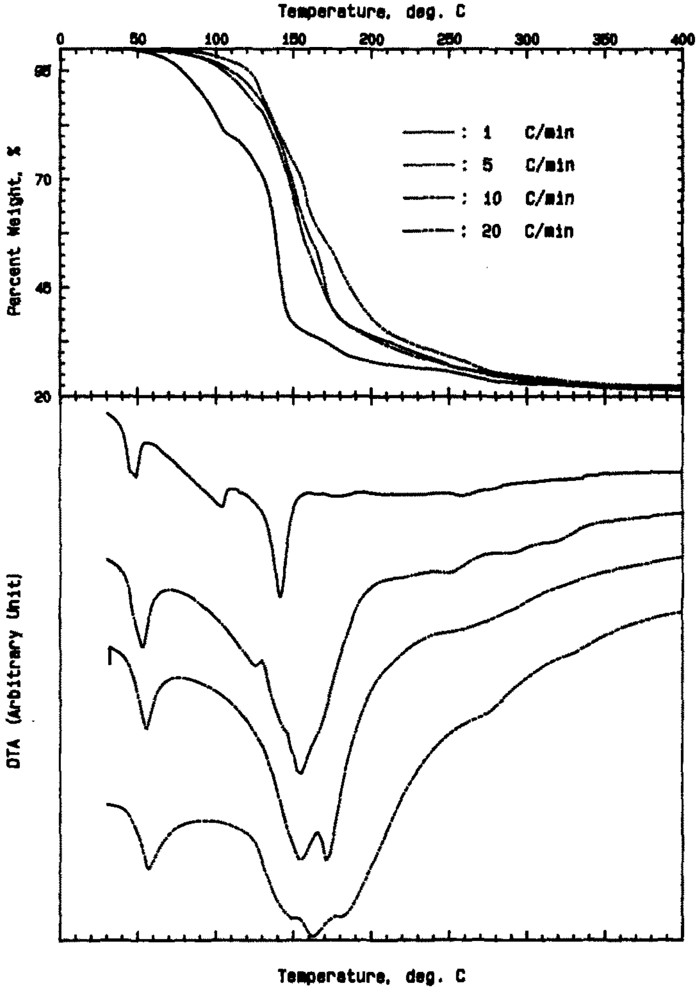

Fig. 6. Thermal behavior of mixed Ni^{II} and Fe^{III} nitrates in stagnant air.

TG curve. The weight of the sample remained constant above 375 ° C. After heating up to 500 ° C, the material had a weak magnetic character and its color was black. This material was composed of crystallites of Fe_2O_3, NiO, and $NiFe_2O_4$ as evident from its X-ray pattern. When the mixed nitrates were heated up to 1500 ° C using a heating rate of 10 ° C min^{-1}, a pure, well crystallized nickel ferrite was obtained. NiO and Fe_2O_3 were not detected by the X-ray diffraction analysis. The formation of $NiFe_2O_4$ from NiO and Fe_2O_3 is not accompanied by a change in weight, but if it occurs over a narrow temperature range a peak should be detected on the DTA curve. No such peak was detected.

To emphasize the conclusion that the behavior of the mixture was an overlap of those weight losses expected to occur in the individual materials, the values for loss in weight at different temperatures for the stoichiometric composition were calculated and then compared with the TG curves obtained for the mixed nitrates. Using a 1°C min^{-1} heating rate in stagnant air, the mixture tended to decompose earlier than the individual nitrates. This phenomena may indicate a fine grain size for the intermediate products obtained from the mixture. Nevertheless, when the analysis was carried out at 20°C min^{-1} with a slow stream of air (10.9 ml min^{-1}), a better agreement between the calculated points and the obtained curve was obtained).

Nickel acetate tetrahydrate

Figure 7 gives the thermal curves for $Ni(CH_3COO)_2 \cdot 4H_2O$ obtained in stagnant air using 1, 5, and 10°C min^{-1} heating rates. After reaching a nearly constant weight, X-ray diffraction analyses confirmed the presence of NiO. Using a heating rate of 1°C min^{-1}, the salt started to lose weight at 65°C. A weight drop of about 30% of the original weight occurred within a temperature increment of 60°C. The rapid weight loss (from 65 to 125°C) was associated with a sharp endothermic peak on the DTA curve. This endothermic reaction represented the dissociation and vaporization of water of crystallization from nickel acetate hydrates. Above 125°C, the rate of weight loss decreased and the composition approached $(1-y)Ni(CH_3COO)_2 \cdot yNi(OH)_2$ with a value for y of 0.116 at 250°C. Above 260°C, a second rapid weight loss was observed. This weight loss occurred between 260 and 375°C and was accompanied by an exothermic effect (as shown on the DTA curve). From the shape of this exothermic peak, it can be concluded that it was due to several overlapping reactions with a net exothermic effect. When a specimen was heated in a muffle furnace, a flame was observed indicating that the decomposition caused evolution of gases (CO and maybe H_2) which oxidize in air with a flame. Above 400°C, no other detectable peak existed on the DTA curve and the weight remained constant. The X-ray diffraction patterns indicated that NiO was formed. Using back calculation, the purity of the starting material was proven to be 99.93%.

Using a heating rate of 5°C min^{-1}, the thermal curves were similar to those obtained at 1°C min^{-1} up to 400°C. Above 400°C, a different feature was observed. The material continued to lose weight. As the temperature reached 483°C, a gain in weight was observed and the composition approached that of NiO at about 733°C. The quenched material between 450 and 550°C had a black color and exhibited magnetic character. The X-ray diffraction pattern for this quenched material showed that it consisted of NiO and metallic Ni. It seems that the evolved gases caused a reducing atmosphere with an oxygen pressure sufficiently low to reduce the material to metallic Ni. The use of heating rates of 5°C min^{-1} and above resulted in

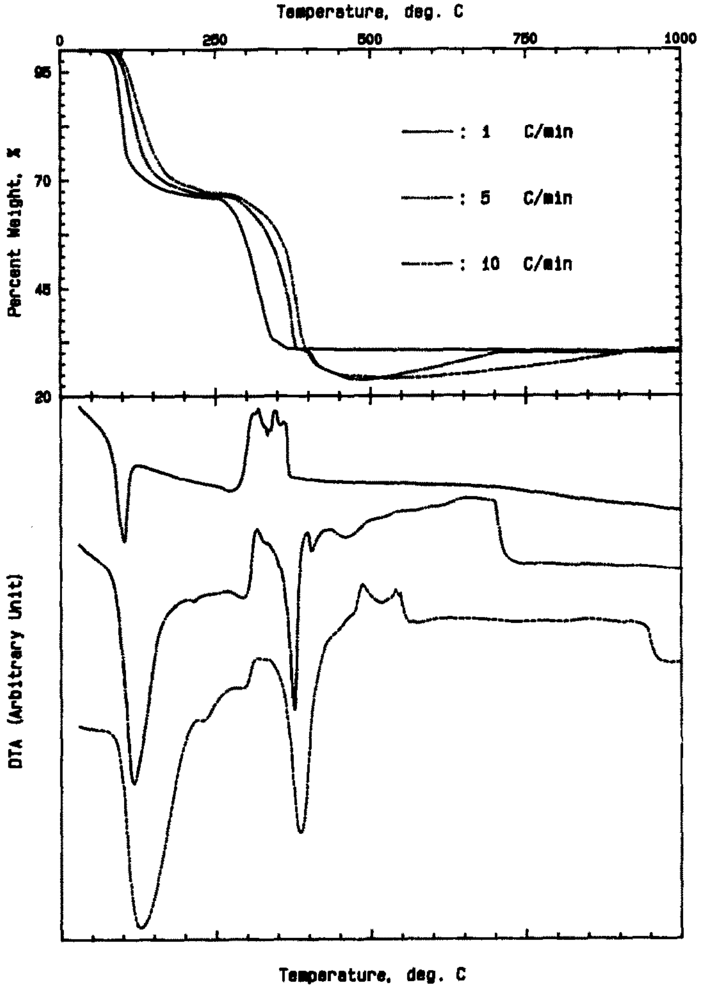

Fig. 7. Thermal analysis of nickel acetate tetrahydrate in stagnant air.

retarding the oxidation of Ni formed. Above 350 °C, a broad exothermic peak was detected on the DTA curve. This exothermic peak was attributed to the oxidation of Ni. A heating rate of 10 °C min^{-1} showed that longer times and higher temperatures were needed to complete the oxidation of Ni to NiO. The steps of the decomposition of nickel acetate at heating rates of 5 °C min^{-1} and above are

$$\mathrm{Ni(CH_3COO)_2 \cdot 4H_2O} \rightarrow (1-y)\mathrm{Ni(CH_3COO)_2} \cdot y\mathrm{Ni(OH)_2}$$
$$\rightarrow z\mathrm{NiO} + (1-z)\mathrm{Ni} \rightarrow \mathrm{NiO} \qquad (3)$$

where the values of y and z depend on heating rate and temperature.

Basic iron(III) acetate

Figure 8 shows the thermal curves for the salt obtained in stagnant air using different heating rates. When a heating rate of 1° C min^{-1} was used, the TG curve showed that $Fe(OH)(CH_3COO)_2$ began to lose weight at around 30° C. A rapid weight loss was observed on the TG curve below 300° C and some endothermic and exothermic transitions corresponding to the loss in weight were observed on the DTA curve. Above 300° C the composition of the salt approached that of Fe_2O_3. The X-ray diffraction analysis confirmed that this material was Fe_2O_3. A reversible weight loss accompanied by an endothermic peak was detected above 1350° C and was associated with the decomposition of hematite to a non-stoichiometric

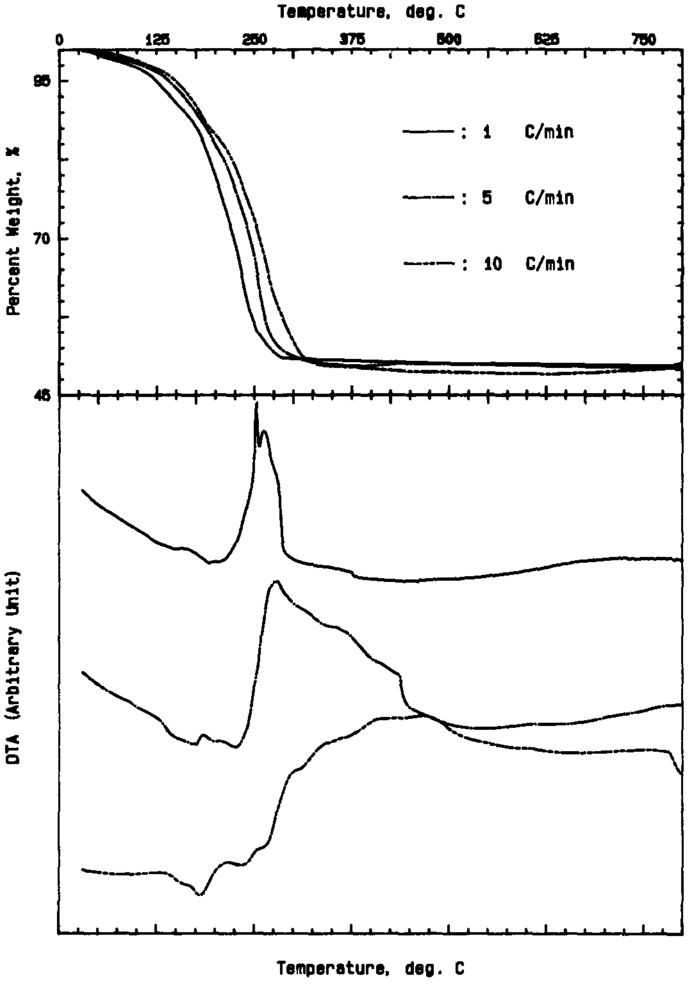

Fig. 8. Thermal analysis of basic ferric acetate in stagnant air.

magnetite. Heating rates of 5 and 10 °C min^{-1} caused these thermal curves to be shifted to higher temperatures. Moreover, the basic ferric acetate decomposed to iron oxide with some iron existing in an oxidation state of less than three. X-ray analysis of an quenched sample indicated the presence of magnetite. Further heating caused the complete oxidation of the material to Fe_2O_3 with pick-up of oxygen. It is evident that with higher heating rates, higher temperatures were required to fully oxidize the iron (Fig. 8).

The steps for the decomposition of basic iron acetate in air can be described as follows.

$$Fe(OH)(CH_3COO)_2 \rightarrow uFe_2O_3 + (1-u)Fe_3O_4 \rightarrow Fe_2O_3 \qquad (4)$$

where u depends on the heating rate and temperature.

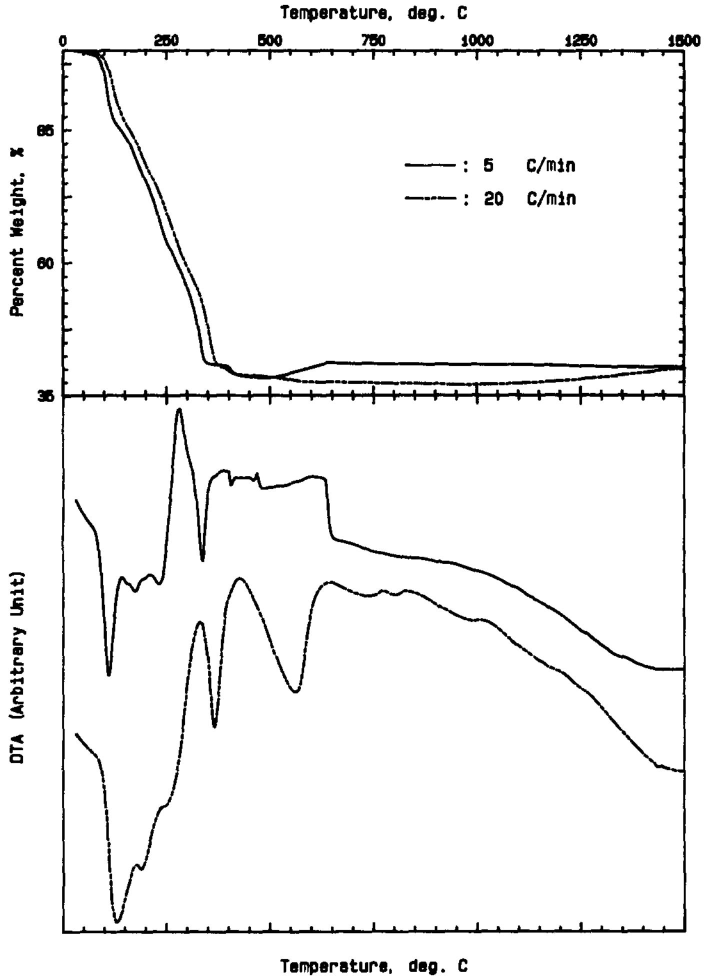

Fig. 9. Thermal analysis of the mixed Ni^{II} and Fe^{III} acetates in stagnant air.

A heating rate of 1° C min^{-1} was slow enough for the complete oxidation to Fe_2O_3 without detecting Fe_3O_4.

Mixed acetates

Nickel acetate tetrahydrate and basic ferric acetate were mixed in the ratio to form $NiFe_2O_4$ and then the mixed acetates were thermally analyzed (see Fig. 9). The curvature on the TG curve at temperatures between 400 and 650° C was mainly due to the reduction of NiO to Ni metal and then the oxidation of Ni to NiO. The final product was $NiFe_2O_4$.

The effect of heating rates on the TG and DTA curves was the same as those observed for the individual salts.

Comparing the behavior of different salts

The results obtained in the present work were compared with those for hydroxides obtained by Gadalla and Livingston [13], see Table 1. All the data summarized in Table 1 are for heating in stagnant air using a heating rate of 10° C min^{-1}.

Considering the decomposition temperature required to form the corresponding oxide and the solubility in water of the salt, nickel and iron nitrates, which have the lowest decomposition temperature range and the high solubility in water, will be the best starting materials for the aerosolization process. The high solubility in water guarantees the homogeneity of the starting solution. The low decomposition temperature is expected to allow for the complete decomposition to the required oxides during the aerosolization process which usually has a very short residence time.

TABLE 1

Summary of the thermal behavior and solubility of some salts of Ni^{II} and Fe^{III}

Material decomposed	Solubility in water	Temperature for forming oxides (° C)	Oxide
$Ni(NO_3)_2 \cdot 6H_2O$	Very soluble	310–375	NiO
$Ni(CH_3COO)_2 \cdot 4H_2O$	Slightly soluble	400–960	NiO
$Ni(OH)_2$ [a]	Insoluble	200–380	NiO
$Fe(NO_3)_3 \cdot 9H_2O$	Very soluble	163–250	Fe_2O_3
$Fe(OH)(CH_3COO)_2$	Insoluble	300–775	Fe_2O_3
α-FeOOH [a]	Insoluble	580–730	Fe_2O_3

[a] Results from Gadalla and Livingston [13].

CONCLUSIONS

Equations (1)–(4) show the decomposition of the salts. When a stream of air was introduced during the decomposition, all decomposition reactions occurred at lower temperatures due to the enhanced removal of the gaseous by-products by the air stream. On the other hand, an increase in heating rate caused the elevation of the decomposition temperatures and a broadening of the peaks on the DTA curves, essentially due to a decrease in homogeneity of temperature inside the material. At high heating rates, nickel nitrate hexahydrate decomposed, with only anhydrous basic nickel nitrate as an intermediate, and iron nitrate nonahydrate tended to decompose directly to the anhydrous hematite. For acetates, the decomposition products created a reducing atmosphere which reduced NiO to the metallic state and iron oxide to magnetite at heating rates above 5 °C min^{-1}. On further heating they oxidized back to NiO and Fe_2O_3 respectively. With higher heating rates, higher temperatures were needed to achieve complete oxidation. The thermal curves obtained for the mixed nitrates and acetates were an overlap of the individual curves of the components and did not reveal the steps of a solid state reaction to form the ferrite or of its crystallization.

ACKNOWLEDGMENTS

We gratefully acknowledge support of this research by the Regents of Texas A & M University through the AUF-sponsored Materials Science and Engineering Program.

REFERENCES

1 W.W. Wendlandt, Texas J. Sci., 10 (1958) 392.
2 D. Dollimore, G.A. Gamlen, and T.J. Taylor, Thermochim. Acta, 86 (1985) 119.
3 D. Dollimore, G.A. Gamlen, and T.J. Taylor, Thermochim. Acta, 91 (1986) 287.
4 J.M. Criado, A. Ortega, and C. Preal, React. Solids, 4 (1987) 93.
5 D. Dollimore, G.A. Gamlen, and T.J. Taylor, Thermochim. Acta, 51 (1981) 269.
6 I.I. Kalinichenko and A.I. Purtov, Russ. J. Inorg. Chem., 11 (1986) 891.
7 J. Mu and D.D. Perlmutter, Thermochim. Acta, 56 (1982) 253.
8 J. Leicester and M.J. Redman, J. Appl. Chem., 12 (1962) 375.
9 D. Dollimore and J. Pearce, J. Therm. Analysis, 6 (1974) 321.
10 P. Baraldi, Spectrochim. Acta, 38 (1982) 51.
11 S. Music, M. Ristic, and S. Popuic, J. Radio. Nucl. Chem., 121 (1988) 61.
12 Introduction to Ceramics, W.D. Kingery, H.K. Bowen, and D.R. Uhlmann (Eds.), Wiley, New York, 1976.
13 A.M. Gadalla and T.W. Livingston, Thermochim. Acta, 145 (1989) 1.